Cathode effects in cylindrical Hall thrusters

E. M. Granstedt,[a] Y. Raitses,[b] and N. J. Fisch[c]
Plasma Physics Laboratory, Princeton University, P. O. Box 451, Princeton, New Jersey 08543, USA

(Received 26 May 2008; accepted 23 August 2008; published online 17 November 2008)

Stable operation of a cylindrical Hall thruster has been achieved using a hot wire cathode, which functions as a controllable electron emission source. It is shown that as the electron emission from the cathode increases with wire heating, the discharge current increases, the plasma plume angle reduces, and the ion energy distribution function shifts toward higher energies. The observed effect of cathode electron emission on thruster parameters extends and clarifies performance improvements previously obtained for the overrun discharge current regime of the same type of thruster, but using a hollow cathode neutralizer. Once thruster discharge current saturates with wire heating, further filament heating does not affect other discharge parameters. The saturated values of thruster discharge parameters can be further enhanced by optimal placement of the cathode wire with respect to the magnetic field. © *2008 American Institute of Physics*. [DOI: 10.1063/1.2999343]

I. INTRODUCTION

The development of efficient miniaturized Hall thrusters for low-power space applications is an active area of research.[1,2] The cylindrical Hall thruster (CHT) concept features a reduced surface-to-volume ratio in comparison to conventional annular Hall thrusters,[3–5] making it potentially more attractive for miniaturization. Other features include quiet operation,[3,4,6] high ionization efficiency,[3,4,7] and a magnetic topology which may reduce channel erosion.[5] These features lead to efficiencies at low power comparable to the state-of-the-art annular Hall thrusters of commensurate size.[6] However, a main shortcoming to the CHT design is the significantly larger divergence of the plasma plume.[3] The half plume angle of a CHT can be as high as 60°–80°,[3] compared to 45°–50° for the best annular Hall thrusters,[8] where the plume angle is defined as the angle that contains at least 90% of the total ion current.[8–10] The resulting anode efficiency is typically 15%–25% in the 100–200 W power range.[11] Radial pressure gradients, magnetic field curvature, and the distribution of ion production all affect the plasma plume divergence.[12,13]

Recent work has demonstrated that the CHT half plume angle can be reduced to 50°–55° by overrunning the discharge current in the input power range of 50–200 W.[11,14] This dramatic narrowing of the CHT plasma plume was coupled with a nearly twofold increase in the fraction of high-energy ions, better focusing of these ions, and a shift of the ion energy distribution function (IEDF) peak (~30 eV) to higher energy.[14] These enhancements resulted in a measured anode efficiency of 30%–40% in the 100–200 W power range.[14] The higher discharge currents necessary to enter this regime were obtained by driving a current between the keeper and the emitter of the hollow cathode neutralizer.[14]

The previous work left open the question of whether the enhanced CHT performance was a consequence of the complex internal physics of the hollow cathode (for example, a non-Maxwellian electron energy distribution function with fast electrons[15,16] and possibly double layers[15,17]) or the coupling between the cathode and near-field plasma plume. To simplify the problem, the hollow cathode neutralizer was exchanged for a resistively heated wire filament. This present study demonstrates that thruster performance can be varied substantially simply by adjusting the cathode electron emission from a thermionic filament.

Section II describes the filament cathode, facility, and thruster operation; Sec. III discusses the experimental results and their implications; Sec. IV summarizes the major findings.

II. EXPERIMENT BACKGROUND

The CHT used in this work has a 3 cm channel diameter and was built to operate at the 100 W power level with 2–4 SCCM (SCCM denotes cubic centimeter per minute at STP) Xenon gas as the propellant (Fig. 1). Details of the design and performance of the thruster are reported elsewhere.[5–7]

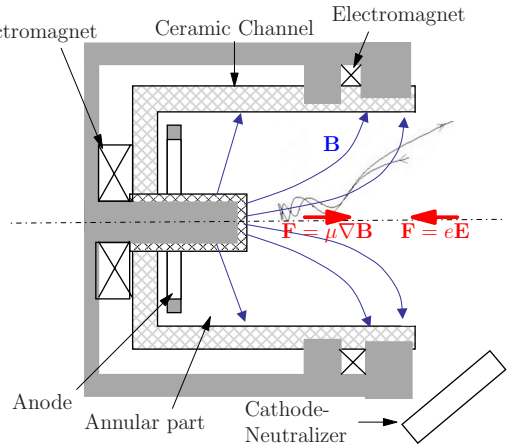

FIG. 1. (Color online) Schematic of the CHT.

[a]Electronic mail: erikg@princeton.edu.
[b]Electronic mail: yraitses@pppl.gov.
[c]Electronic mail: fisch@pppl.gov.

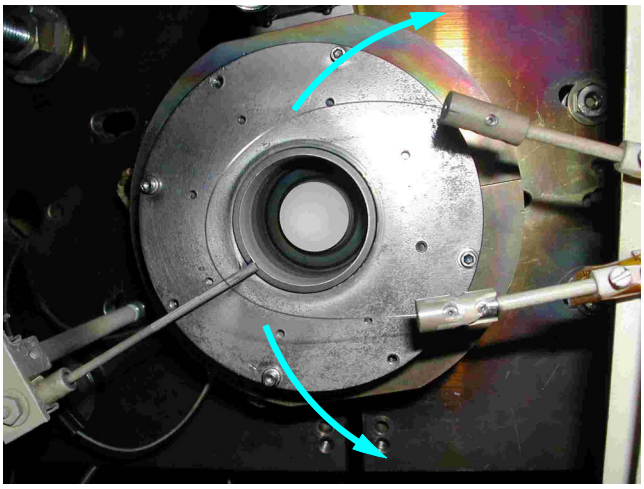

FIG. 2. (Color online) Filament assembly and floating probe mounted to the CHT. Thruster channel diameter is 3 cm. Floating probe at left is positioned just past the channel exit, nearly flush with the channel. Filament assembly at right holds four filaments and can be rotated to bring other filaments into position. The filament wire loop can be rotated in a fixed axial plane (indicated by the arrows in the figure) so that part of the loop crosses the thruster channel.

In the present study, the thruster was operated in the "direct" configuration: currents in the front and back coils are codirected, resulting in an enhanced axial magnetic field.[6] A voltage of 250 V was applied between the thruster anode and cathode, and the entire thruster assembly was electrically floating with respect to the grounded vacuum chamber walls.

The cathode filament was constructed from a 13.5 cm long loop of 0.25 mm diameter thoriated tungsten wire. The 1% Thorium increases electron emission as compared with Tungsten, by decreasing the work function.[18] The calculated filament lifetime was tens of hours based on evaporation, but actual lifetime was expected to be significantly less due to ion bombardment. To enable extended thruster operation without opening the vacuum vessel, a filament holder assembly was constructed that held four filaments and allowed a new one to be rotated into place after a failure. In practice, filament lifetime ranged from 15 min to several hours. Measurements of filament temperature using an optical pyrometer provided a calibration with heating current. The Richardson–Duschman equation ($J=AT^2e^{-\Phi/T}$, $\Phi_{W-Th}=2.7$ eV, $A=4$ A cm^{-2} K^{-2}) (Ref. 18) gave an expected source electron emission up to several amperes, assuming emission from the entire filament surface and typical heating powers of 50–130 W (filament temperatures from 1650–2200 K) used in this study. The filament was positioned in a plane about 2 cm beyond the thruster channel exit (Fig. 2).

The ion angular distribution was measured by a negatively biased 1 cm^2 planar graphite probe with a guarding sleeve.[19] The electrically isolated guarding sleeve serves to mitigate edge effects due to the sheath and ensure the probe is collecting only from the planar surface. The probe was located 15 cm from the thruster channel exit and rotated $\pm 90°$ relative to the thruster axis to measure plume divergence.[7]

The probe and sleeve were biased to −40 V with respect to the grounded chamber walls, sufficient to repel plasma electrons and measure only ion saturation current.

Ion charge exchange with the surrounding background gas is known to distort the ion current angular distribution measured by planar probes: slow neutrals ionized by charge exchange are accelerated by the potential gradient of the plume and contribute to the measured ion current at large angles.[20–22] To quantify this effect with each angular scan of the ion flux probe, the smallest current measured at $\pm 90°$ was taken to be an upper bound on the contribution from background ions to the ion current measurement.[7]

The plume angle was then approximated as the average of that computed with and without subtracting this maximum background ion contribution, with half of the difference taken as the uncertainty.

A four-grid retarding potential analyzer[23] (RPA) was used to measure the IEDF near the thruster centerline and located about 50 cm from the thruster channel exit. The RPA was calibrated with an electrostatic ion source and tested to determine the optimal grid voltages. The first grid was held floating, the second biased to −7 V (with respect to ground) to repel plasma electrons, the third biased with an oscillating 0–400 V positive voltage to filter ions, and the fourth grid was biased to −20 V to block secondary electrons generated by ion impact with the first two grids. During calibration, a −16 V bias of the collector plate was found to minimize current from secondary electrons. This collector bias was therefore used during experiments. Transmission through all the RPA grids was ≈2%. A floating probe, constructed from 0.75 mm diameter graphite and housed in an alumina and boron nitride sleeve, was placed at the thruster channel exit.

The CHT was operated at 2 SCCM Xe, a reduced flow rate compared with previous experiments in the large vacuum chamber, in order to maintain the background pressure below 20 μTorr.

The mean free path for ion charge exchange on background neutrals[24] was $\lambda_{cx}^{in}=v_i/(n_a\langle\sigma_{cx}^{in}v_i\rangle)=280$ cm for 200 eV ions, characteristic of those produced in the thruster. A maximum background pressure of 20 μTorr was chosen so that the probability that a plume ion would undergo charge exchange before it reached the ion flux probe ($1-\exp(-l/\lambda_{cx}^{in})\approx 0.05$) was nearly identical to previous experiments in the large thruster facility conducted at a higher flow rate (4 SCCM through the anode and 2 SCCM through the hollow cathode). The probability of an ion-neutral elastic scattering[25,26] event before reaching the ion flux probe ($1-\exp(-l/\lambda_{el}^{in})\approx 0.3$, where $\lambda_{el}^{in}=v_i/(n_a\langle\sigma_{el}^{in}v_i\rangle)=40$ cm) is also comparable in the two experimental conditions. Therefore, measurements of the plasma plume divergence using the reduced flow rate could be compared to previous results in the lower background pressure environment.

Stable operation was achieved at this flow rate with 1.0 A current through the rear magnetic coil and 2.0 A through the front coil. The resulting magnetic configuration is shown in Fig. 3. These operating parameters were used for all the measurements presented in this paper.

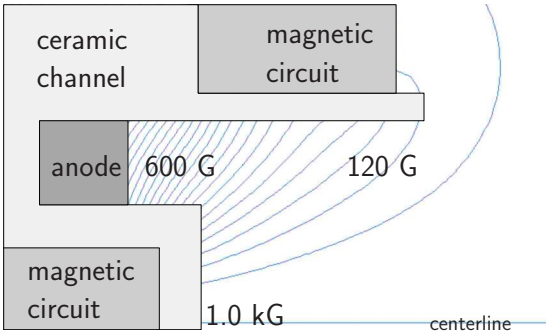

FIG. 3. (Color online) Magnetic field configuration: 2.0 A back coil current, 1.0 A front coil current, and codirected for enhanced axial magnetic field.

III. RESULTS AND DISCUSSION

Significant plume narrowing was achieved simply by increasing electron emission from the hot wire cathode through additional heating. Thus, the performance enhancements reported previously[14] using a hollow cathode were apparently due to the increased emission from the electron source when operating in an electron source-limited regime.

The thruster discharge current was seen to increase with filament heater current up to saturation. The range over which variation of source heating affected the discharge current is understood as a source-limited regime, in contrast to the saturated region where variation of the source heating did not affect thruster parameters. Increased discharge current (while holding gas flow rate, discharge voltage, and magnetic field constant) resulted in a narrower plume and higher ion energy, consistent with the overrun discharge current regime reported previously.

Once discharge current saturation was achieved, further increase in the filament heater current did not result in improved performance. Typically, the plume and ion energy would remain unchanged, although at several instances, the discharge current actually decreased slightly. Generally when the heater current was reduced and the discharge current stabilized at a lower value, the enhanced performance did not persist; however, occasionally hysteresis or a finite persistence of the enhanced performance was observed.

The thruster plume angle did not appear to transition sharply, but rather was gradually reduced 5° (from 62° to 57°) as discharge current increased 10%, from ≈210 to 230 mA (Figs. 4 and 5). Plume angles as high as 66° were measured at low discharge currents. Current utilization[8,27] $[\eta_I = I_{\text{ion}}/I_d = I_{\text{ion}}/(I_{\text{electron}}+I_{\text{ion}})]$, however, decreased from 63% to 59% with discharge current (Fig. 6). This is explained by the increased electron current from the filament, and because unlike prior experiments using a hollow cathode, the total ion current did not change considerably.

The IEDF measured by the RPA shifted ≈15 eV to higher energy with increased discharge current (Fig. 7). Although the enhanced ion energy was correlated with an increased cathode potential −3 to −1 V, this change does not account for the much larger ion energy increase (Fig. 8). Likewise, the minimal (2.5 V) change in the floating potential at the channel exit indicated that if electron temperature remained approximately constant, the change in voltage drop

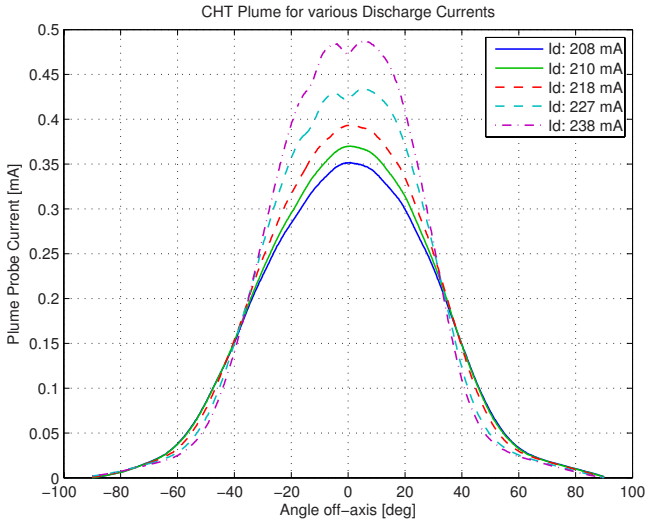

FIG. 4. (Color online) Plume narrowing with increased discharge current (I_d) from higher filament heater current (I_d: 208, 210, and 218 mA) and/or optimized filament positioning (I_d: 227 and 238 mA). Ion flux angular distribution measured with a graphite probe. Thruster centerline corresponds to 0°.

across the channel was also far too small to account for the higher ion energy. An alternative explanation is that ionization inside the thruster channel was taking place at higher plasma potential.

The position of the hot wire cathode was found to be another factor which affected the thruster discharge. Successful startup of the discharge occasionally required adjustment of the wire location. In addition, the value of the saturated discharge current depended sensitively on the position of the wire cathode. This appears consistent with experiments on annular thrusters that have found thruster performance improvement by optimal position of the cathode neutralizer.[28–30]

The filament was typically positioned to be approximately symmetric around the thruster channel (as in Fig. 2), but when the filament wire loop was moved in the fixed axial

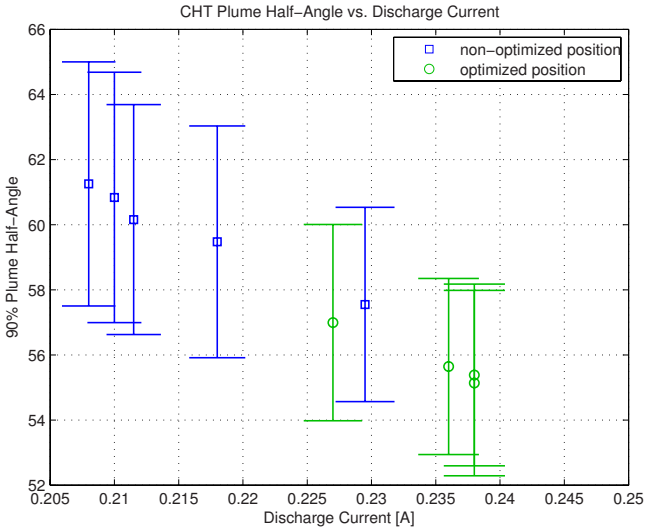

FIG. 5. (Color online) Reduction in plume half-angle with increased discharge current as the filament cathode heating is increased.

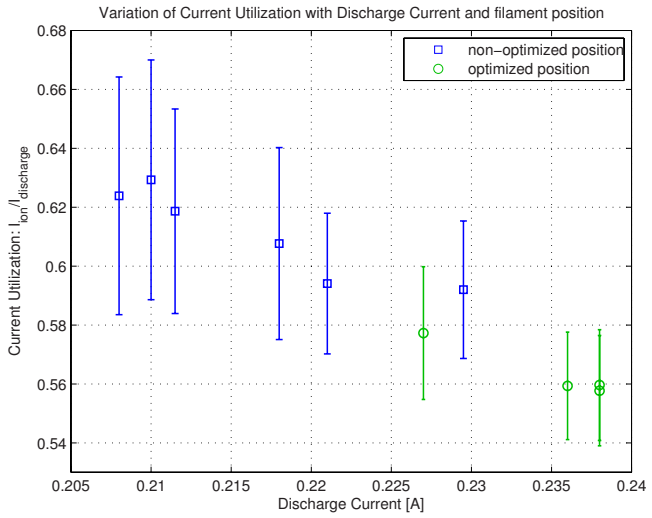

FIG. 6. (Color online) Change in current utilization ($\eta_I = I_{ion}/I_{discharge}$). Errorbar corresponds to the difference in ion current measured with and without background subtraction.

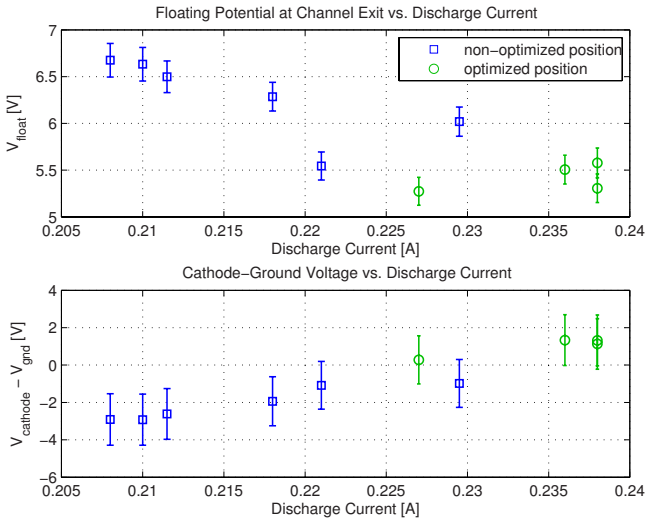

FIG. 8. (Color online) Variation in floating potential at channel exit and cathode coupling voltage (ϕ_{gnd}-ϕ_{cath}) with discharge current. Floating potential at the channel exit decreased only very slightly relative to the 250 V discharge voltage or 11–22 V drop across the filament. The change in the cathode coupling voltage does not sufficiently account for the measured ion energy increase.

plane, the saturated discharge current increased gradually as part of the wire loop approached the thruster centerline. The saturated discharge current achieved its maximum of ≈240 mA when part of the wire loop approximately intersected the thruster centerline. This position of maximum saturated discharge current is referred to as the "optimized position" in Figs. 4–8. The thruster plume angle was also reduced a further 2° (to 55°), and accompanied by an additional ≈15 eV increase in the mean ion energy (Figs. 5 and 7).

It is important to note that although the additional influence of the cathode position on the discharge characteristics appeared to be qualitatively similar to what has been observed in annular thrusters,[28,29] the magnetic field distribution in the CHT was very different (see Figs. 1 and 3). The greater discharge current achieved when the cathode wire crossed the thruster axis suggests that optimal position of the cathode (from the standpoint of a narrower plume) may be determined by the insertion of electrons along magnetic field lines in the hybrid magnetic mirror and electrostatic trap (Figs. 1 and 3).

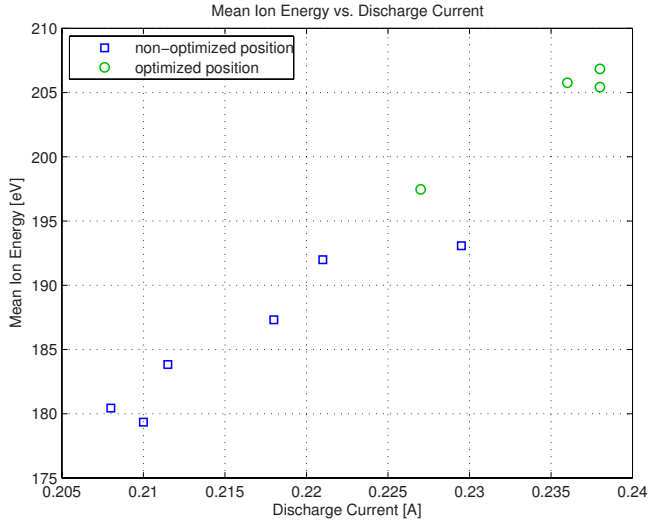

FIG. 7. (Color online) Increase in mean ion energy with discharge current as filament heating is increased. Saturated discharge current and ion energy were increased further when the filament cathode was positioned to cross the thruster centerline. The full width at half maximum of the IEDF is typically ~20 eV.

The measured ion energies and plume angles at discharge current saturation were reproducible to within 1 eV and 1° of those presented here, even after extended operation with different filament wires. Over the course of several days of experiments, a continuous increase in the electron contribution to the discharge current was observed. This 15%–20% increase in discharge current is consistent with the buildup of a conductive coating on the ceramic channel walls produced by evaporation of the tungsten wire.

The measured performance enhancement of the CHT with increased filament heating is consistent with previous measurements using the 3 cm thruster with a hollow cathode neutralizer at a higher flow rate: plume narrowing from 62° to 50° and a shift in the peak of the IEDF ~30 eV to higher energy.[14]

At high filament heater currents with the filament crossing the thruster channel, the average cathode potential was measured as high as ≈1 V above the grounded chamber walls. A virtual cathode potential dip near the cathode filament[31] provides a possible explanation for this abnormality. Since the thermionic emission current was generally larger than the discharge current, a potential well due to excess electron space charge may have been present near the filament to reduce the effective electron emission:

$$\phi_{cath} - \phi_{min} \approx eT_c \ln\left(\frac{I_{emission}}{I_d}\right) \approx 0.7 \text{ V}.$$

This potential dip would be adequate to place the potential minimum near ground. Although negative potential wells may be destroyed by the buildup of slow charge exchange ions,[31] in this case, the time for charge exchange ions[24] to

accumulate in the negative potential well around the filament $(\nu_{cx}^i)^{-1} \sim (n_0 \langle \sigma_{cx}^i v_i \rangle)^{-1} \gtrsim 150$ μs was substantially longer than the time for ions to be accelerated to the filament supports. This ion loss time was on the order of the filament length (~10 cm) over the ion velocity gained from the potential gradient along the filament ($\gtrsim 10$ V), $\tau_{\text{loss}}^i \sim L/\sqrt{eV/m_i} \lesssim 40$ μs. Therefore, ions were accelerated along the length of the filament, eventually contacting the filament supports before a sizeable number of slow ions could build up to dominate the behavior of the virtual cathode potential dip.

In other experiments operating with high filament heating currents and the filament wire crossing the thruster channel, however, the cathode potential was measured to be as high as several volts above ground. The position of electron emission from the cathode in the magnetic field geometry may also contribute to the shifted cathode potential, but the mechanisms are not understood.

IV. CONCLUSION

The cathode electron emission current strongly influenced the performance of the CHT. In addition, the position of the cathode with respect to the mirror-like magnetic field of the CHT was another parameter that affects thruster performance. From a macroscopic standpoint, the characteristics of the thruster discharge did not appear to depend on the internal physics of the electron source except to the extent the attainable electron current is modified; in particular, a filament cathode could produce thruster plumes and ion energy distributions similar to those generated when a hollow cathode neutralizer was used. Specifically, performance enhancements of the overrun current regime reported previously have been attained using a filament cathode. At relatively low discharge currents, the thruster was operated in an electron source-limited regime, where discharge current increased with filament heater current. In this regime, thruster performance also improved gradually: the plume angle was reduced and the on-axis mean ion energy increased with discharge current. Once discharge current saturation occurred, however, subsequent increase in filament heater current did not improve thruster performance. The saturated value of discharge current was sensitive to the position of the electron source, with a higher value achieved when the filament crossed across the thruster channel.

Since the enhanced ion energy could not be explained entirely by changes in the cathode potential or the voltage drop in the thruster channel, further work is necessary to understand how ion acceleration in the thruster channel is modified by varying cathode emission. In particular, measurements of plasma potential and density inside the thruster channel may determine whether ionization is taking place in a region of higher potential. Finally, the specific mechanisms that are affected by cathode emission to decrease plasma plume divergence remain to be identified.

ACKNOWLEDGMENTS

The authors thank Artem Smirnov for helpful discussions and to Enrique Merino and Martin Griswold for their technical assistance.

This work was supported by grants from AFOSR and U.S. DOE Contract No. AC02-76CH0-3073. One of us (E.M.G.) wishes to acknowledge the support of a DOE Fusion Energy Sciences Graduate Fellowship.

[1] D. Courtney and M. Martínez-Sánchez, Proceedings of the 30th International Electric Propulsion Conference, Florence, Italy, 2007, IEPC Paper No. 2007-39.
[2] V. Khayms and M. Martínez-Sánchez, *Progress in Astronautics and Aeronautics* (AIAA, Reston, VA, 2000), Vol. 187, p. 47.
[3] Y. Raitses and N. J. Fisch, Phys. Plasmas **8**, 2579 (2001).
[4] A. Shirasaki and H. Tahara, J. Appl. Phys. **101**, 073307 (2007).
[5] A. Smirnov, Y. Raitses, and N. Fisch, IEEE Trans. Plasma Sci. **34**, 132 (2006).
[6] A. Smirnov, Y. Raitses, and N. J. Fisch, J. Appl. Phys. **92**, 5673 (2002).
[7] A. Smirnov, Y. Raitses, and N. J. Fisch, J. Appl. Phys. **94**, 852 (2003).
[8] R. R. Hofer, R. S. Jankovsky, and A. D. Gallimore, J. Propul. Power **22**, 732 (2006).
[9] Y. Raitses, D. Staack, A. Dunaevsky, and N. J. Fisch, J. Appl. Phys. **99**, 036103 (2006).
[10] N. J. Fisch, Y. Raitses, L. A. Dorf, and A. A. Litvak, J. Appl. Phys. **89**, 2040 (2001).
[11] A. Smirnov, Y. Raitses, and N. J. Fisch, Phys. Plasmas **14**, 057106 (2007).
[12] A. Fruchtman and A. Cohen-Zur, Appl. Phys. Lett. **89**, 111501 (2006).
[13] M. Keidar and I. D. Boyd, Appl. Phys. Lett. **87**, 121501 (2005).
[14] Y. Raitses, A. Smirnov, and N. J. Fisch, Appl. Phys. Lett. **90**, 221502 (2007).
[15] D. Goebel, K. Jameson, R. Watkins, I. Katz, and I. Mikellides, J. Appl. Phys. **98**, 113302 (2005).
[16] I. Mikellides, I. Katz, D. Goebel, and J. Polk, J. Appl. Phys. **98**, 113303 (2005).
[17] N. Plihon, P. Chabert, and C. Corr, Phys. Plasmas **14**, 013506 (2007).
[18] W. H. Kohl, in *Handbook of Materials and Techniques for Vacuum Devices*, American Vacuum Society Classics (American Institute of Physics, New York, 1995).
[19] W. Lochte-Holtgreven, in *Plasma Diagnostics*, American Vacuum Society Classics (AIP, New York, 1995).
[20] D. H. Manzella and M. Sankovic, Proceedings of the 31st AIAA/ASME/SAE/ASEE Joint Propulsion Conference and Exhibit, San Diego, CA, 1995, AIAA Paper No. 1995-2927.
[21] M. L. R. Walker, A. Victor, R. Hofer, and A. Gallimore, J. Propul. Power **21**, 408 (2005).
[22] Y. Azziz, N. Z. Warner, and M. Martínez-Sánchez, Proceedings of the 40th AIAA/ASME/SAE/ASEE Joint Propulsion Conference and Exhibit, Fort Lauderdale, Florida, 2004, AIAA Paper No. 2004-4097.
[23] A. Dunaevsky, Y. Raitses, and N. J. Fisch, Appl. Phys. Lett. **88**, 251502 (2006).
[24] J. S. Miller, S. H. Pullins, D. J. Levandier, Y. Hui Chiu, and R. A. Dressler, J. Appl. Phys. **91**, 984 (2002).
[25] A. V. Phelps (ftp://jila.colorado.edu/collision_data/).
[26] A. V. Phelps, J. Appl. Phys. **76**, 747 (1994).
[27] V. Kim, J. Propul. Power **14**, 736 (1998).
[28] J. D. Sommerville and L. B. King, Proceedings of the 30th International Electric Propulsion Conference, Florence, Italy, 2007, IEPC Paper No. 2007-78.
[29] D. L. Tilley, K. H. de Grys, and R. M. Myers, Proceedings of the 35th AIAA/ASME/SAE/ASEE Joint Propulsion Conference and Exhibit, Los Angeles, CA, 1999, AIAA Paper No. 99-2865.
[30] R. R. Hofer, L. Johnson, D. Goebel, and D. Fitzgerald, Proceedings of the 42nd AIAA/ASME/SAE/ASEE Joint Propulsion Conference and Exhibit, Sacramento, CA, 2006, AIAA Paper No. 2006-4482.
[31] T. Intrator, M. H. Cho, E. Y. Wang, N. Hershkowitz, D. Diebold, and J. DeKock, J. Appl. Phys. **64**, 2927 (1988).